JAERI-M
8273

SEISMIC RESPONSE ANALYSIS FOR PRISMATIC FUEL HTGR CORE

June 1979

Takeshi IKUSHIMA

日本原子力研究所
Japan Atomic Energy Research Institute

この報告書は，日本原子力研究所が JAERI-M レポートとして，不定期に刊行している研究報告書です．入手，複製などのお問合わせは，日本原子力研究所技術情報部（茨城県那珂郡東海村）あて，お申しこしください．

JAERI-M reports, issued irregularly, describe the results of research works carried out in JAERI. Inquiries about the availability of reports and their reproduction should be addressed to Division of Technical Information, Japan Atomic Energy Research Institute, Tokai-mura, Naka-gun, Ibaraki-ken, Japan.

JAERI-M 8273

Seismic Response Analysis for Prismatic Fuel HTGR Core

Takeshi IKUSHIMA
Division of Power Reactor Projects,
Japan Atomic Energy Research Institute

(Received May 15, 1979)

For high-temperature gas cooled reactors (HTGR) with prismatic fuels, their resistance against an earthquake is not fully ascertained yet. Aseismic design studies and also experiments must therefore be made when such a reactor plant is to be installed in areas of high seismicity.

This report describes analytical study on the seismic response of a prismatic fuel reactor core, including the following: aseismic core structure, the analysis model and calculation formulae, the effects of various design variables on response characteristics, and the desired block shape.

Three analysis models have been considered for the seismic vibration of the prismatic fuel HTGR core. The first is the impact model, the second "the spring dashpot model", and the third "the dryfriction model". The calculation has been performed with three models, and these results are nearly the same.

The followings were revealed: (1) At low input-wave frequencies, the response value increases with the gap between the blocks. Beyond a certain point, however, the effect of gap is nearly negligible. (2) When the blocks are restrained horizontally by keys, the response value decreases with increase of the key stiffness. The key is thus effective in earthquake resistance. (3) The response value increases with block-stiffness, so that short massive blocks are better for earthquake resistance. (4) The response value decreases with increase of the block damping factor. But beyond a certain point, this effect is only small. (5) Stiffness and damping in the restraint structure for the reactor core do not have much effect in earthquake resistance.

Keywords: HTGR Core, Seismic Response, Prismatic Fuel, Seismic Analysis, Aseismic Design, Graphite Core, Earthquake Resistance Design, VHTR Core, Stiffness, Damping

JAERI－M 8273

ブロック状燃料炉心高温ガス炉の地震応答解析

日本原子力研究所・動力炉開発安全性研究管理部
幾島　毅

（1979年5月15日受理）

ブロック状燃料高温ガス炉の炉心の耐震性は十分に確保されていない。それ故，この炉が地震国に建設される場合，十分な耐震研究が心要とされる。

本報は，ブロック状炉心の地震応答解析に関するものであり，内容は，炉心耐震構造，解析モデルと計算式，振動特性に及ぼす種々の設計変数の影響，望ましいブロック形状である。

3つの解析モデルがブロック状燃料高温ガス炉炉心の地震振動のため考慮された。第1は衝突モデル，第2はスプリング・ダッシュポケットモデル，第3は乾摩擦モデルである。計算は3つのモデルについて実施され，これらの結果はほとんど同じ応答値を示した。

解体結果から次のことが明らかになった。

(1) 低周波数入力加振において，応答値はブロック間ギャップの増加に従って増加する。

(2) ブロックは互にキー結合された場合，応答値はキーの剛性増加に従って減少する。それ故，キーは耐震上望ましい。

(3) 応答値はブロックの剛性増加に従って増加する。それ故，短く太いブロックが耐震上有効である。

(4) 応答値はブロックの減衰定数の増加とともに減少する。しかし，ある値以上になるとこの効果は変らなくなる。

(5) 炉心拘束構造物の剛性値と減衰値の変化による影響はわずかである。

目　　次

Contents

1. Introduction

In a gas-cooled reactor core, graphite is used as the main structural material. Graphite, compared with steel, is fairly brittle with a low breaking strength, and besides its thermal expansion coefficient is small. The thermal expansion coefficient of graphite is about one thirds that of steel. Since the periphery of the reactor core is made of steel, provision must be made for absorbing the difference in thermal expansion between the steel periphery and graphite core. And by exposure to the fast neutrons, it undergoes appreciable dimensional change. This dimensional change is then approximately -1 to -2% during the fuel life time. In consequence, the graphite blocks continue to reduce in size during reactor operation, and the meantime, the gap between blocks increases steadily. Moreover in a high-temperature gas cooled reactor (HTGR), fuel and moderator are embodied in a block (or fuel element), so that in fuel exchange, the block itself must be removed. There then arises the need for its easy replacement. During the lifetime of the reactor in operation, the tight assemblage is thus difficult, so that the usual practice is their arrangement with gap in horizontal direction. Under this situation, however, structural integrity of such "loose" reactor core, at the time of a major earthquake, has not been confirmed yet.

Reactor so far with the block-type fuel have been or are being constructed on the seismic zones with none or little seismicity, and so seismic response analysis or other consideration were hardly made on their design. In this connection, for the unit I of the Japan Atomic Power Company (JAPC) Tokai power station in Japan, the vibration test with a simulated reactor core was made, but only to confirm integrity of the reactor core.[1)]

One of the most difficult problems in the design of a block-type fuel HTGR is in its aseismic construction. The vibration tests and analyses of core are now performing in the General Atomic Company (GAC).[2),3)] In the Japan Atomic Energy Research Institute (JAERI), design studies for the Experimental Multi-purpose HTGR were started about 5 years ago, and main emphasis has been on its aseismic aspect.

In the present report, descriptions were, concerned to the block-type fuel core, calculation models and formulae, effects on vibration of that core various variables, including between-blocks gap, input acceleration wave, between-blocks stiffness, between-blocks and-support-plate stiffness, restraint-structure, block stiffness, block damping factor, restraint-structure damping factor, and friction, and finally the desired block shape.

2. Structure of Reactor Core

The block-type fuel core of a HTGR is such as in Fig.1, which shows the HTGR being developed in JAERI. The reactor core is enclosed in a core barrel, horizontally restrained at the top with an orifice block of a heat-resisting alloy, while the bottom is restrained similarity with a core support plate through keys. Then in the periphery, the core is restrained by the core barrel. Fuel blocks in the core are generally connected together in vertical direction with three dowel pins, but in the horizontal direction they are loose with gap between them.

Concerning the horizontal arrangement, as shown in Fig.2, one type is not restrained at all, while the other is restained by key and keyway. Nuclear and thermal characteristic are better in the former type than in the latter. Moreover, manufacture of the blocks with key and keyway is difficult. As thus seen, if integrity of the block-type fuel core against an expected major earthquake in the installation area can be retained without the key and keyway, the loose type is far better.

In the periphery of a block-type fuel core, the fixed reflector in block form adjoins the core barrel certain restraint. In the unit I of the JAPC's Tokai power station and the Fort St. Vrain reactor, restraint bars penetrate through the fixed reflector, thereby transmitting seismic force from the reactor core to the external barrel.[4] Integrity of this scheme in an earthquake is going to be confirmed, and it is incorporated in the large HTGR and preliminary design of the Experimental Multi-purpose HTGR.[5]

3. Analysis Model and Formulae

3.1 Model

In the block-type fuel core, this group of blocks extends in so-called three dimensions as shown in Fig.3. In the present study, the following simplified models as shown in Fig.3 through 8 for calculation will be considered.

(1) The blocks at the top are restrained the orifice block with some stiffness and damping.

(2) The blocks at the bottom are restrained the core support plate with some stiffness and damping.

(3) The blocks are restrained three dowels and dowel pins with some stiffness and damping.

(4) The blocks in the core periphery are restrained with the restrained structure with some stiffness and damping.

(5) Frictions exist between blocks as shown in Fig.7.

(6) It can be conceivable two models for the mass of blocks:

(i) each blocks are lumped mass (L-mass type),

(ii) each blocks are consistent mass (C-mass type).

(7) It can be conceivable three models for the impact phenomena as shown in Fig.6:

(i) spring dashpot model (S-impact type),

(ii) impact model (I-impact type),

(iii) dryfriction model (D-impact type).

(8) Six calculation models can be conceivable according to above (6) and (7) combination. That are:

(a) L-S model (Lumped mass-Spring dashpot type model)

(b) L-I model (Lumped mass-Impact type model)

(c) L-D model (Lumped mass-Dryfriction type model)

(d) C-S model (Consistent mass-Spring dashpot type model)

(e) C-I model (Consistent mass-Impact type model)

(f) C-D model (Consistent mass-Dryfriction type model).

3.2 Formulae

3.2.1 General Formulae

In Fig.3 through 8 the equation of motion for block i; at the core center, with its position in absolute coordinate as Y, is then given as,

$$C_{i1}(\dot{Y}_i - \dot{Y}_1) + K_{i1}(Y_i - Y_1) - C_{ki}(\dot{Y}_k - \dot{Y}_i) - K_{ki}(Y_k - Y_i) \pm F_{fil} \pm F_{fki} = - m_i\ddot{Y}_i + F_p \qquad (1)$$

where, F_p is the force from surrounding mass points. With y as the local coordinate from the core barrel instead of Y, and hence $y_i=Y_i-Y_o$, eq.(1) takes the following form:

$$m_i\ddot{y}_i + C_{i1}(\dot{y}_i - \dot{y}_1) + K_{i1}(y_i - y_1) - C_{ki}(\dot{y}_k - \dot{y}_i) - K_{ki}(y_k - y_i) \pm F_{fil} \pm F_{fki} = - m_i\ddot{y}_o + F_p \qquad (2)$$

in eqs.(1) and (2) suffix zero mean the core barrel, and hence, evidently $y_o=Y_o$. The equation of motion for a block i adjoining the core barrel, with stiffness coefficient and damping coefficient of the restraint structure as K_{Bi} and C_{Bi} respectively, is similarly given as,

$$m_i\ddot{y}_i + C_{Bi}\dot{y}_i + K_{Bi}y_i + C_{i1}(\dot{y}_i - \dot{y}_1) + K_{i1}(y_i - y_1) - C_{ki}(\dot{y}_k - \dot{y}_i) - K_{ki}(y_k - y_i) \pm F_{fij} \pm F_{fki} = - m_i\ddot{y}_o + F_p \qquad (3)$$

3.2.2 Spring Dashpot Model

In eqs.(2) and (3), if the mass i is in coupled state with its surrounding masses, F_p are given as,

$$F_p = -\left\{ \sum_j C_{ij}(\dot{y}_i - \dot{y}_j) + \sum_j K_{ij}(y_i - y_j + \delta_{ij}) \right\} \tag{4}$$

and

$$F_p = -\left\{ \sum_j C_{ij}(\dot{y}_i - \dot{y}_j) + \sum_j K_{ij}(y_i - y_i + \delta_{ij}) \right\} \tag{5}$$

Concerning the effect of gap between blocks, as shown in Fig.8 the three different models are conceivalbes.

(1) Model-A: no restraint in the gap

In Fig.8(a), when the two adjoining masses i and j, adhere together, there exist stiffness coefficient K_{ij} and damping coefficient C_{ij} in eqs.(4) and (5). And if they do not, both the values are zero.

$$\left.\begin{aligned} K_{ij} &= C_{ij} = 0 \quad : y_i - y_j \geq -\delta_{ij} \\ K_{ij} &= k_{ij} \\ C_{ij} &= C_{ij} \quad : y_i - y_j < -\delta_{ij} \\ \delta_{ij} &= \delta_{ij} \end{aligned}\right\} \tag{6}$$

(2) Model-B: some restraint in the gap

In Fig.8(b), when the masses i and j adhere or do not, the K_{ij} and C_{ij} in eqs.(4) and (5) take the corresponding different values.

$$\left.\begin{aligned} K_{ij} &= K_{ij}^{(1)},\ C_{ij} = C_{ij}^{(1)} \\ \delta_{ij} &= 0 \end{aligned}\right\} : y_i - y_j \geqq -\delta_{ij}$$

$$\left.\begin{aligned} K_{ij} &= K_{ij}^{(2)},\ C_{ij} = C_{ij}^{(2)} \\ \delta_{ij} &= \delta_{ij}^{(2)} \end{aligned}\right\} : y_i - y_j < -\delta_{ij} \qquad (7)$$

(3) Model-C: some restraint in the gap with limitation

In Fig.8(c), if the two masses adhere or do not, the K_{ij} and C_{ij} in eqs.(4) and (5) are different, correspondingly. When the masses i and j are separated beyond a certain distance, however, both the values become zero.

$$\left.\begin{aligned} K_{ij} &= C_{ij} = 0 && : y_i - y_j \geqq 0 \\ K_{ij} &= K_{ij}^{(1)},\ C_{ij} = C_{ij}^{(1)} \\ \delta_{ij} &= 0 \end{aligned}\right\} : 0 > y_i - y_j \geqq -\delta_{ij}^{(2)}$$

$$\left.\begin{aligned} K_{ij} &= K_{ij}^{(2)},\ C_{ij} = C_{ij}^{(2)} \\ \delta_{ij} &= \delta_{ij}^{(1)} \end{aligned}\right\} : y_i - y_j < \delta_{ij}^{(2)} \qquad (8)$$

As seen, above equations are non-linear, and of these three models, Model-A can applied to the motion of blocks when there exists some gap between them in horizontal direction. And Model-B and C are applicable to the case when the adjoining blocks are joined together with key and keyway.

(4) Compressive Force in Block

With the stiffness coefficient between blocks as K_{ij} and restraint in the gap, the force acting on the mass points i and j with gap δ is given as,

$$\left.\begin{aligned} P_{ij} &= 0 && : \text{if } y_i - y_j \geqq \delta_{ij} \\ P_{ij} &= K_{ij}(y_i - y_j + \delta_{ij}) && : \text{if } y_i - y_j < \delta_{ij} \end{aligned}\right\}, \qquad (9)$$

the compressive force at one side of a block is P_{ij}. When it is compressed on both sides, however, the total compressive force in the block is $P_{ij}+P_{ki}$, where P_{ki} is that due to block k on the other side.

(5) Stiffness Coefficient in Block

The equivalent stiffness coefficient of a block when this block adheres to the adjoining blocks, is that values when it is compressed. It can thus be obtained from the Yong's modulus of graphite. For a solid block of sectional area A and width B, the compressive force it receives when subjected to strain $\Delta B/B$ is given as,

$$F = \frac{EA\Delta B}{B} \quad . \tag{10}$$

The stiffness coefficient K is $F/\Delta B$. For the block, it can be obtained as,

$$K = \frac{EA}{B} \quad . \tag{11}$$

3.2.3 Impact Model[6)]

In the impact model, the impulse and momentum technique for the collision is used. Velocity and the collision force after collision are calculated from the impulse-momentum equation.

$$\left.\begin{aligned} V_{il} &= \frac{(m_i V_{io} + m_j V_{jo}) - em_j(V_{io} - V_{jo})}{m_i + m_j} \\ V_{jl} &= \frac{(m_i V_{io} + m_j V_{jo}) + em_i(V_{io} - V_{jo})}{m_i + m_j} \\ F &= \frac{(V_{jD} - V_{iD})(1 + e)}{t_c} \cdot \frac{m_i m_j}{m_i + m_j} \end{aligned}\right\} \tag{12}$$

3.2.4 Dryfriction Model[7)]

This model is a combination of Impact and Spring dashpot model. In eqs.(2) and (3), F_p are given as

$$F_p = \begin{cases} K_{ij}(y_i - y_j) + \dfrac{K_{ij}(1 - e)}{1 + e}(y_i - y_j) : \dot{y} \geqq 0 \\ K_{ij}(y_i - y_j) - \dfrac{K_{ij}(1 - e)}{1 + e}(y_i - y_j) : \dot{y} \leqq 0 \end{cases} \quad (13)$$

3.2.5 Relation between Coefficient of Restitution and Damping Coefficient[8)]

The relation between the coefficient of restitution and the damping coefficient will be given on the assumption (see Chapter 4).

3.2.6 Comparison of Impact Model

The calculation has performed with above three models, and these results are nearly the same as shown in Fig.9.

4. Assumptions in Analysis

(1) Mass and Stiffness of Blocks and Gap between Blocks

Response values of the reactor core are influenced by those of the reactor building, pressure vessel, and etc. To observe vibration characteristics of the core alone, it is therefore desirable to disregard these effects. The system is thus assumed to consist only of the core and its enclosing barrel.

As shown in Fig.10, it is a series of thirteen blocks horizontally for the Experimental Multi-purpose HTGR; the block-type fuel core is surrounded with barrel and support plates. The weight, stiffness coefficient and damping factor for these blocks and restraint bars are shown in Table 1 and a sample calculation is shown in Fig.11.

The gap between blocks is initially 1 mm at room temperature. With residence in the reactor core, however, they reduce in size due to fast neutron irradiation, so that the gap between blocks increases. For the fast-neutron dose of $1.5 \times 10^{21} n/cm^2$, the shrinkage of graphite blocks is about 1%. If the diameter (between the opposite sides) of a hexagonal block is about 300 mm, the dimensional change is thus 3 mm. The gap between blocks at room temperature can be assumed to be a maximum of 4mm.

(2) Input Acceleration Wave and Maximum Acceleration

For the input acceleration at the core barrel, the sine wave will be used. The natural frequency of reactor core structures and the predominant frequency in an earthquake are usually in the vicinity of 10 Hz, so that in the present analysis this value is used as the frequency of sine wave.

From the results of calculation, maximum acceleration of the core

barrel is known to be up to about three times as large as that of the building foundation. If the latter value is 350 gal, therefore, the maximum accelaration at the core barrel is then 1000 gal. The value of 350 gal for the foundation may be taken as maximum possible in the reactor sites in Japan; 1000 gal for the barrel is convenient for comparison purposes.

(3) Duration Time of Response Calculation

From the results of calculation, for a periodic acceleration wave the maximum response acceleration is seen to occur during the computation time of about 1 sec, in the frequency range of 3 to 20 Hz.

(4) Numerical Solution[9)]

To obtain numerical solutions of the vibration equations from (4) to (8), either the Runge-Kutta-Gills or the Hamming-Predictor-Corrector methods may be used. The former will be employed, since it may give less error in calculations.

(5) Damping Factor and Coefficient of Restitution Relationship

When collision body would be considered to be elasto-plastic model, the following relation are seen between coefficient of restitution e and damping coefficient C.

$$E = \exp(-h\omega t) \tag{14}$$

where,

$$\left.\begin{aligned} h &= \frac{C}{C_c} \\ C_c &= \sqrt{2mk} \end{aligned}\right\}$$

$$\left.\begin{aligned} \omega &= \sqrt{\frac{k}{m}} \\ t &= \frac{\pi}{\omega\sqrt{1-h^2}} \end{aligned}\right\} \qquad (15)$$

The relationship between coefficient of restitution and critical damping factor is derived from eqs.(14) and (15) and is shown in Fig.12.

Coefficient of restitution has been measured experimentally shown in Fig.13 using a pendulum device, which two hexagonal graphite block are collided each other. In the Figure, coefficient of restitution decrease with increasing of impact velocity. HTGR core configuration, maximum impact velocity is assumed below 100 cm/sec, so that coefficient of restitution is about 0.6 from Fig.13. An impact damping factor of 10% of the critical was used in this analysis.

5. Results and Discussion

In the paper, the calculation has performed with Lumped mass-Coupled type model. The following were revealed.

(1) Effect of Number of Block

Effect of number of block in one-dimensional array on response is analyzed in the cases of three, seven, thirteen, twenty-one and thirty-one blocks' array shown in Fig.14. In the figure, values can be arranged as a function of the maximum displacement of blocks, and it is seen that number of blocks have slightly effect on response values.

The following results obtained in the case of thirteen blocks, therefore can be applied for vibration characteristics of any number of blocks.

(2) Response Acceleration and Force Relationship

The response acceleration and impact force of blocks are shown in Fig.15 as a function of the input frequency. From this Figure, the impact force is proportional to the response acceleration.

The tendency of impact force can be seen from the response acceleration.

(3) Effect of Gap between Blocks

The relation between gap and response acceleration is shown in Fig.16. In the input-wave frequency range of 1 to 3 Hz, the response acceleration increases with increase of the clearance between blocks. Then in the range of 4 to 10 Hz, the occurrence of a maximum response acceleration shifts to shorter gap values. Beyond 10 Hz, the influence of clearance on the response is little, being nearly negligible. The tendency described is also observable for response velocity and compressive stress in the blocks.

The phenomena described may be attributed to differences in phase of the impact and the acceleration-force directions when the two adjoining blocks impinge against each other.

(4) Effect of Acceleration-wave Frequency

Figure 17 shows the relation between wave frequency and response values, with total gap as 4.8cm. Displacement of the blocks is hardly influenced by the wave frequency. The response value increase, however, with the frequency in the range of 0.2 to 3 Hz, and maxima appear in the vicinity of 3 Hz. Beyond this frequency, the values decrease gradually. These phenomena, again, may be caused by the phase difference already indicated. The frequency value for the maxima in Fig.11 is not of a resonance, since the natural frequency of blocks is several thousand Hz while the input frequency is only several Hz.

(5) Effect of Stiffness between Blocks

The key connection between blocks may be beneficial in the respect of earthquake resistance. Therefore, response characteristics in the restrained case were examined, using calculation model-C in Fig.8. Figure 18 shows the relation of between-blocks stiffness and the response values. The values decrease with increase of the stiffness, thus indicating the advantage of key and keyway joining of the blocks. This scheme, however, has also many drawbacks, as already described, including the difficulty in fuel exchange due to non-uniform dimensional change by neutron irradiation. Therefore, studies in this respect must be carried out before employment of the joining mechanism.

(6) Effect of Stiffness between Blocks and Core Support Plate

In the prismatic fuel core, the blocks at lowest position are

restrained with the support plate, using key and keyway. The relation of this stiffness and the response values in blocks shown in Fig.19. The values decrease with increase of the stiffness, indicating advantage in earthquake resistance.

(7) Effect of Stiffness of Core Restraint Structure

The displacement of blocks decreases with increase of the restraint structure stiffness. As shown in Fig.20, however, the maximum acceleration (velocity and stress also) are hardly changed. This is because of the maxima is due to impingement between blocks; it depends mainly on the stiffness of blocks, and not on that of the restraint structure.

(8) Effect of Damping Factor of Blocks

The response acceleration initially decreases with increase of the damping factor as shown in Fig.21, but beyond 0.1 the decrease is only little. The damping factor of blocks, as already described, varies with the stress in blocks, so that the actual situation may be different from the present case. Response accelerations for the damping factor below 0.1 must be studied carefully.

(9) Effect of Damping Factor of Core Restraint Structure

Figure 22 shows the effect of restraint structure damping factor on the response acceleration. The value is hardly changed by the damping factor. This is because, as the maximum acceleration occures by impingement between blocks.

(10) Effect of Block Stiffness

For the same weight of blocks, response acceleration increases with increase of the stiffness coefficient as shown in Fig.23; and vice versa. That is to say, those blocks with less stiffness coefficient are

desirable for earthquake resistance. Then, to reduce the stiffness coefficient for a block of constant weight will now be considered. In eq.(11), it is seen that the stiffness coefficient of a block is proportional to its length; so the massive block is better for the current problem.

(11) Effect of Random Mass and Stiffness of Blocks

The weight and stiffness coefficient of respective blocks in thus far calculations differ from one block to another, as in the actual block-type cores. This situation will then be compared with the case of blocks of constant weight and stiffness coeffeicient. Figure 24 summarizes the results obtained in this connection. In the figure, the solid lines show response accelerations for the constant weight and stiffness coefficient, while the confines by broken lines are those for random values. It should noted here that the response accelerations for the latter case are within the boundaries of the former, i.e. constant weight and stiffness coefficient case. The vibration characteristics for a block-type fuel core with random weights and stiffness coefficients can thus be grasped by observation on the case with constant weight and stiffness coefficient.

(12) Effect of Friction between Block and Core Plate

In the calculations thus far, the friction between block and core plate is not considered. Friction exists in the actual core, and there are two types of it, i.e. static and dynamic. It will be assumed here that the two types of friction are of the same value for convienience of calculations.

Figure 25 shows the effect of friction on the response. In Fig.25 the equivalent friction factor (EFF) is the ratio of friction force F_{fi}

to acting force on the blocks due to maximum input acceleration $m_i\ddot{y}_o(max)$:

$$EFF = \frac{F_{fi}}{m_i\ddot{y}_o(max)} \quad . \tag{16}$$

The response values increase with the EFF and maxima appear in the vicinity of 1. Beyond this point, the values decrease rapidly. If EFF is larger than 1, friction is generally desirable to reduce the response values.

6. Conclusions

Calculation models and formulae were presented in order to make seismic response analysis for the block-type fuel core with gap between blocks in horizontal direction. And as the result of calculation, the following were revealed.

(1) In the low range of input wave frequencies, the response acceleration increases with increase of the gap between blocks. At higher frequencies, occurence of maximum value then shifts to lower values of the gap. Beyond a certain point, however, the effect of between-blocks gap is almost negligible.

(2) The response value increases with input wave frequency, and reaches a maximum at a certain point; it then decreases gradually.

(3) When the blocks are restrained horizontally such as key and keyway, the response value decreases with increase of this between-blocks stiffness. This mechanism by key and keyway is thus beneficial in earthquake resistance.

(4) Response values in the vicinity of the core support plate become smaller, the higher stiffness between blocks and the plate.

(5) Stiffness in the restraint structure influences little the response acceleration, velocity and compressive stress, with the exception of block displacement.

(6) The response value decreases with increase of the block damping factor. But beyond 0.1, there is only little effect.

(7) The damping factor in the restraint structure has only little effect on the response value of blocks.

(8) The response value increase with stiffness of the blocks. Their stiffness is thus better to be small for the constant weight; and vice versa.

(9) The response values of a block core with random weight and stiffness of the blocks are within the values for smallest and largest blocks.

(10) The response value changes with the friction force, but the larger friction force is generally not desirable for the aseismic structure.

Mechanical properties will change along with irradiation dose, therefore in the detailed calculation, this effect should be taken into account, in addition the effects stated above.

Acknowledgement

The author wishs to thank Dr. M. Nozawa of Japan Atomic Energy Research Institute for his encouragement.

[Nomenclature]

C : Damping coefficient

e : Coefficient of restitution

F : Force

F_f : Friction force

h : Damping factor, $2h\omega = C/m$

K : Stiffness coefficient

m : Mass of block

t_c : Contact time

v_{io} : Velocity before collision

v_{il} : Velocity after collision

Y : Displacement in absolute coordinate

y : Displacement from core barrel

$\dot{Y}$, $\dot{y}$: Velocity

$\ddot{Y}$, $\ddot{y}$: Acceleration

δ : Gap between blocks

ω : Natural frequency, $\omega = \sqrt{K/m}$

Table 1 Weight, stiffness, and damping factor of blocks

No. of block	Block weight (kg)	Block stiffness (kg/cm)	Damping factor (—)
1 ~ 13	100.0	5×10^6	0.1
Core restraint	10.0	0.5×10^6	0.01

References

1) Muto, K., Bailey, R.W. and Mitchell, K.J.: Design of Nuclear Power Stations to With-stand Earthquakes, Proc. Instn. Mech. Engrs. Vol.177 No.1.

2) NEYLAN, A.J.: Design Development of the HTGR Core and Its Support Structure-Seismic Considerations, 2nd SMiRT (Berlin) K6/7 (1973).

3) BERRIAUD, C. et al.: Experimental and Analytical Studies of HTR Core Seismic Response, 2nd SMiRT (Berlin) K6/8 (1973).

4) Fort St. Vrain Nuclear Generating Station Preliminary Safety Analysis Report (1966).

5) JAERI: First Preliminary Design of Experimental Multi-Purpose High-Temperature Reactor, JAERI-M 4419 (1971).

6) NEYLAN, A.J. and GORHOLT, W.: Design Development of the HTGR Core and Its Support Structure Seismic Considerations, Nucl. Eng. Design Vol.29.

7) NUNO, H. et al.: A Method of Colliding Vibration Analysis of PWR Fuel Assemblies under Seismic Condition, 2nd SMiRT (Berlin) K6/10 (1973).

8) IKUSHIMA, T.: JAERI-M 5560 (1974).

9) IKUSHIMA, T.: PRELUDE-2: Seismic Response Analysis Code for Block-Type Fuel Core, LA-TR-75-9 (1975).

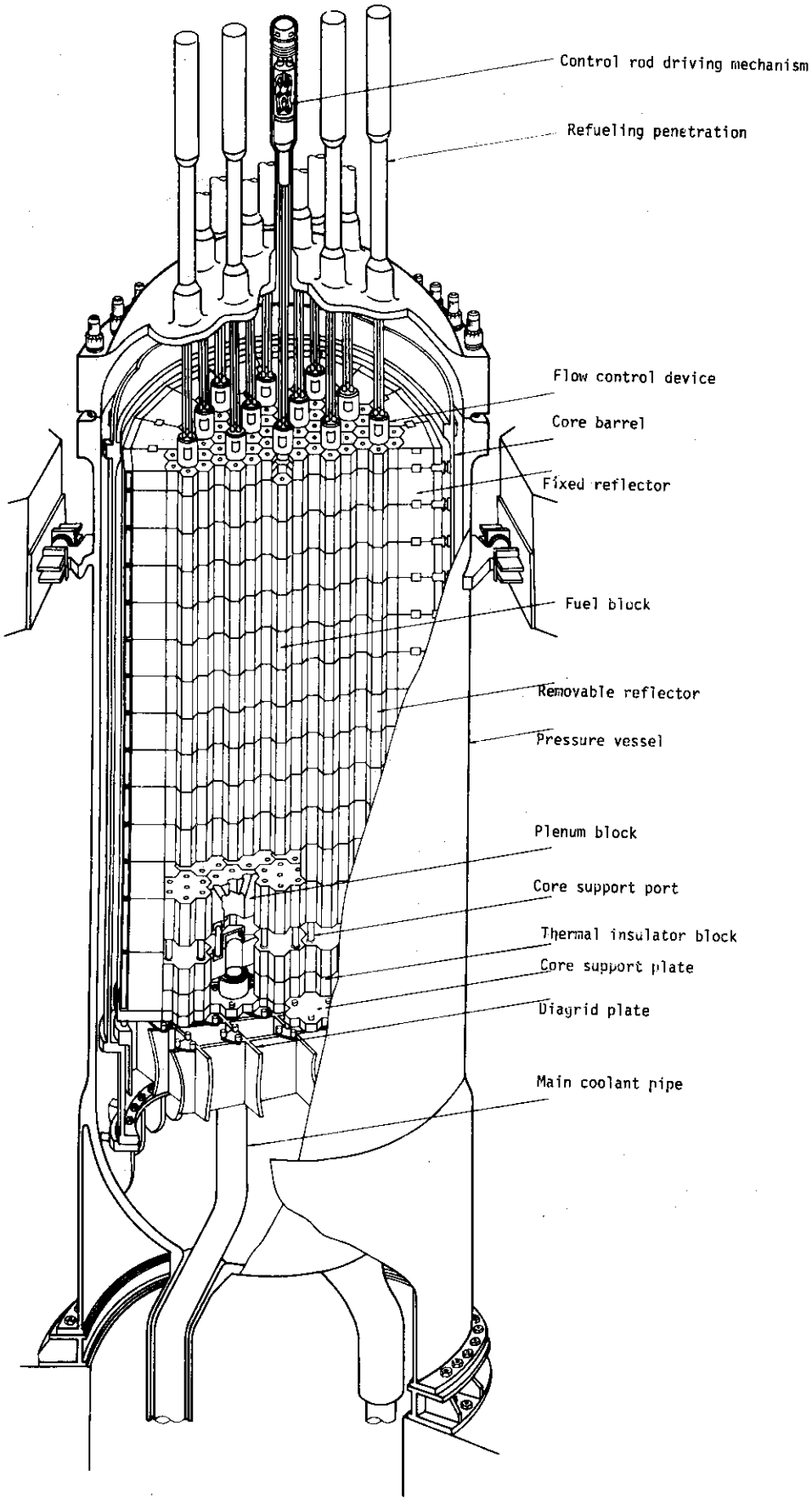

Fig. 1 Reactor vertical view of VHTR

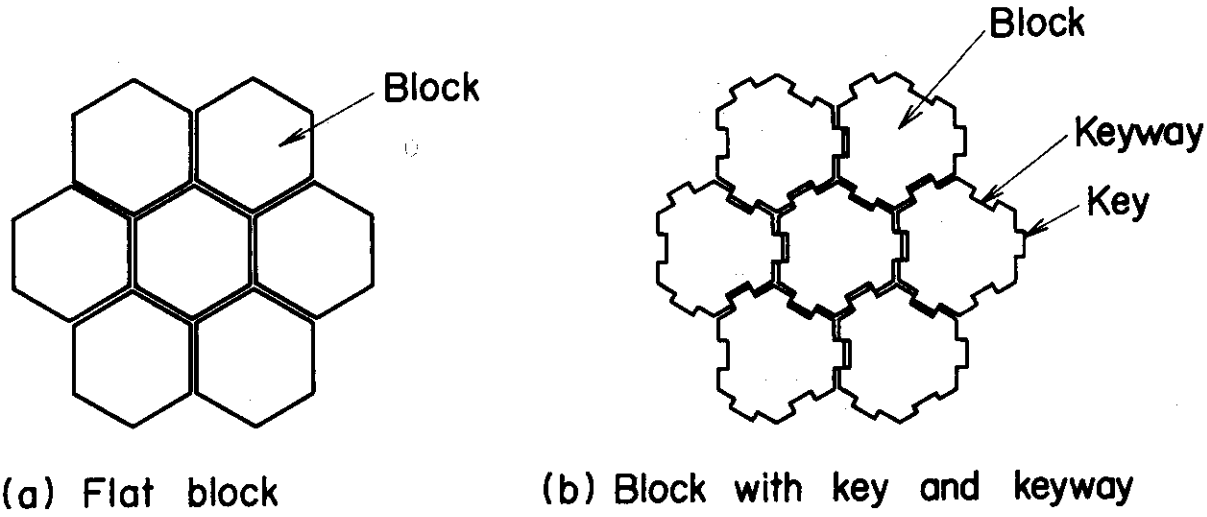

Fig. 2 Fuel element arrangement

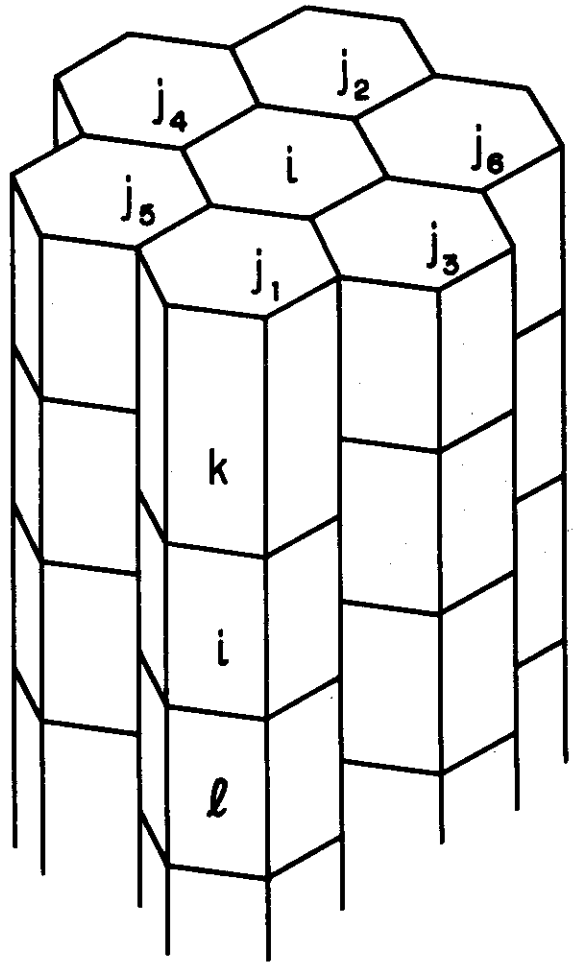

Fig. 3 Block array

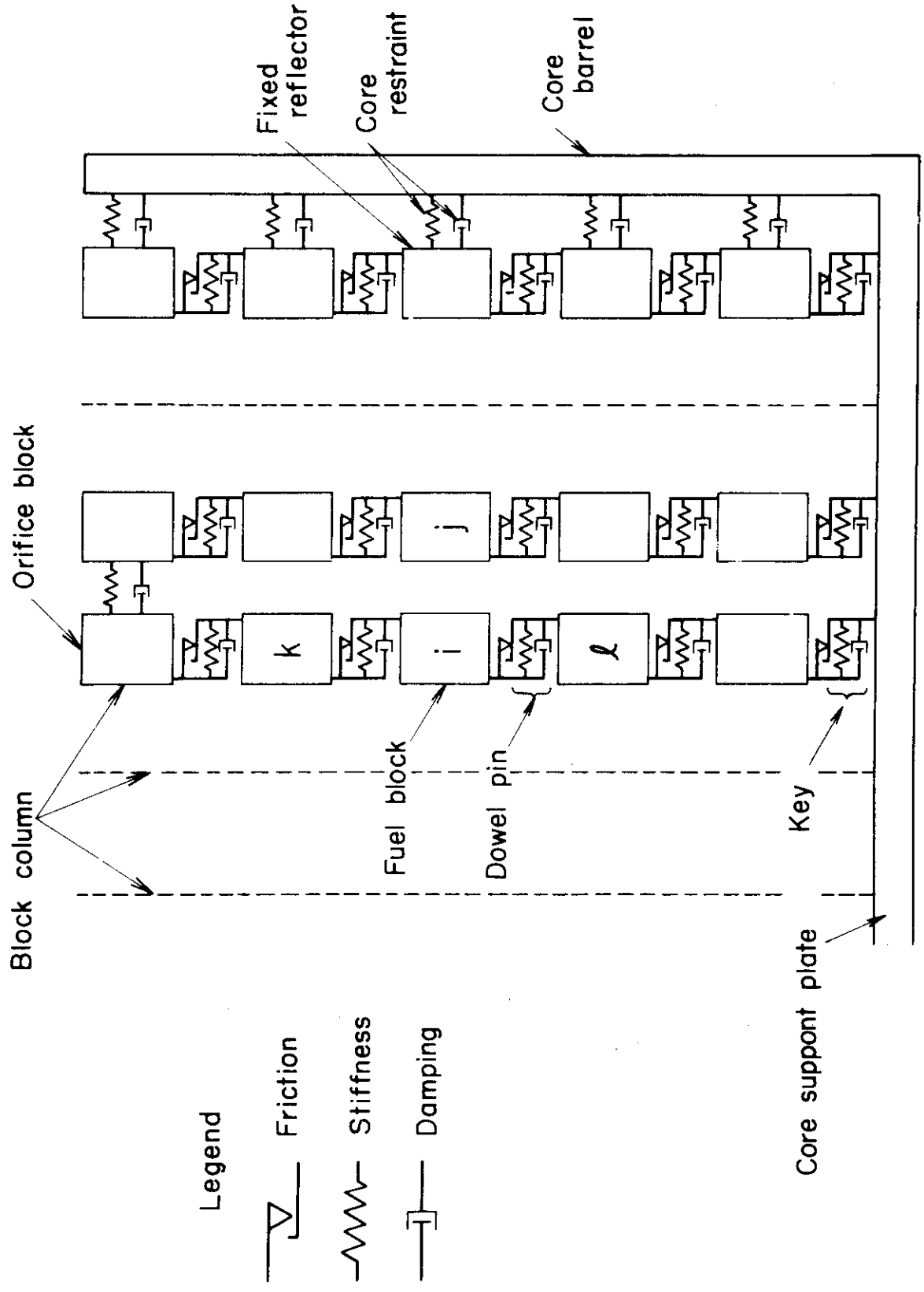

Fig. 4 2-D calculation model for seismic response analysis of HTGR vertical sliced core

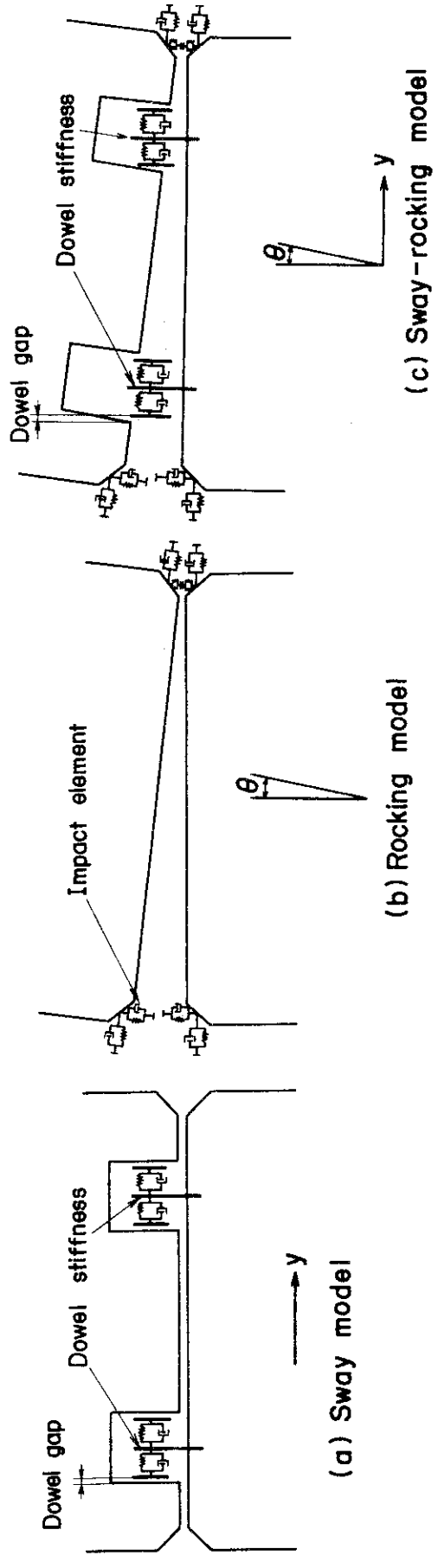

Fig. 5 Block motion model

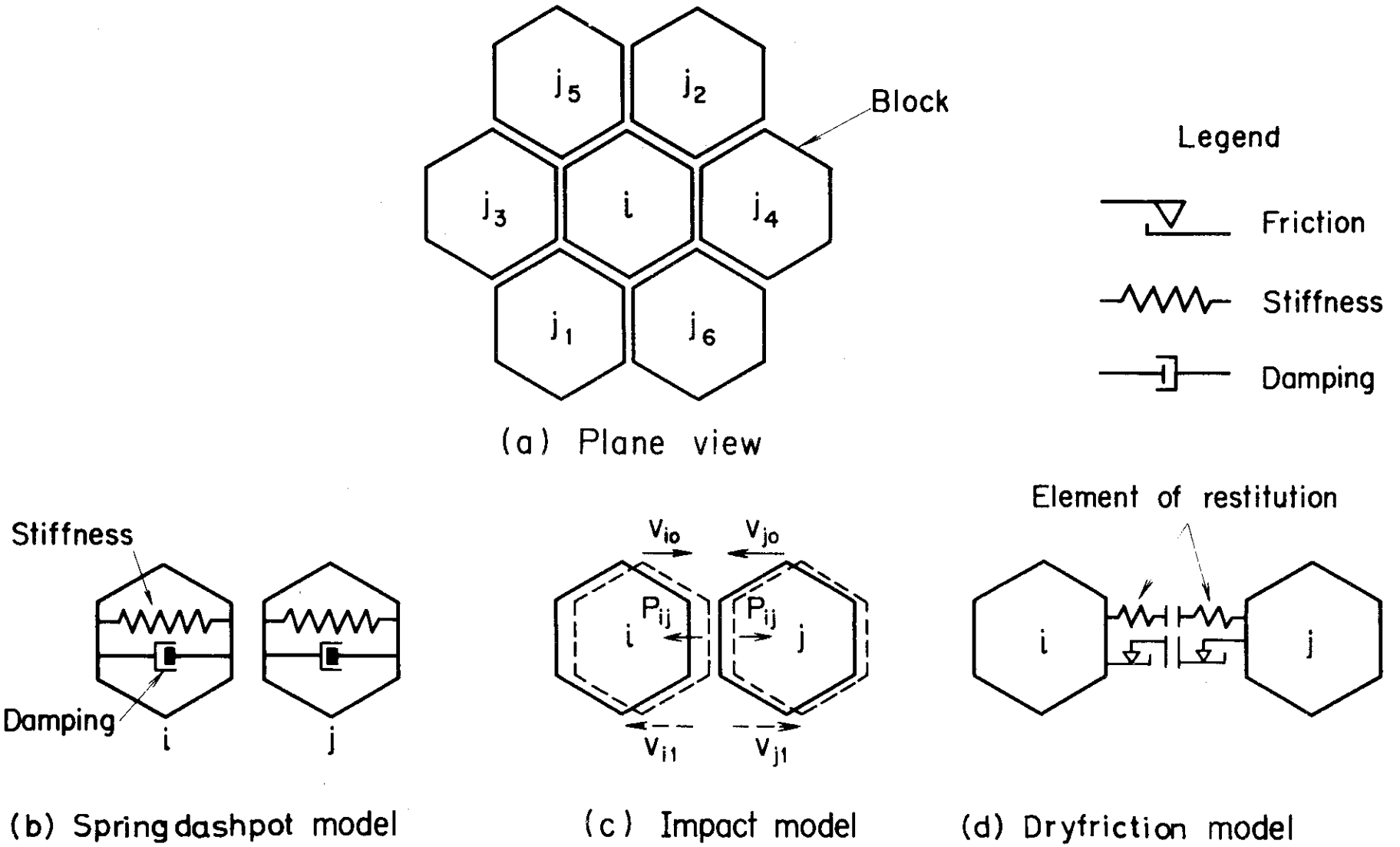

Fig. 6 Block plane arrangement and calculation models

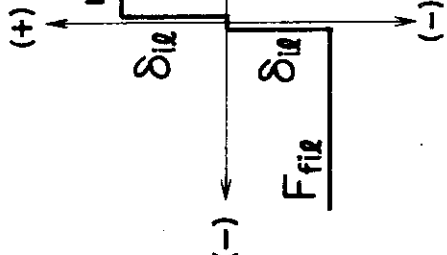

Fig. 7 Calculation model for friction

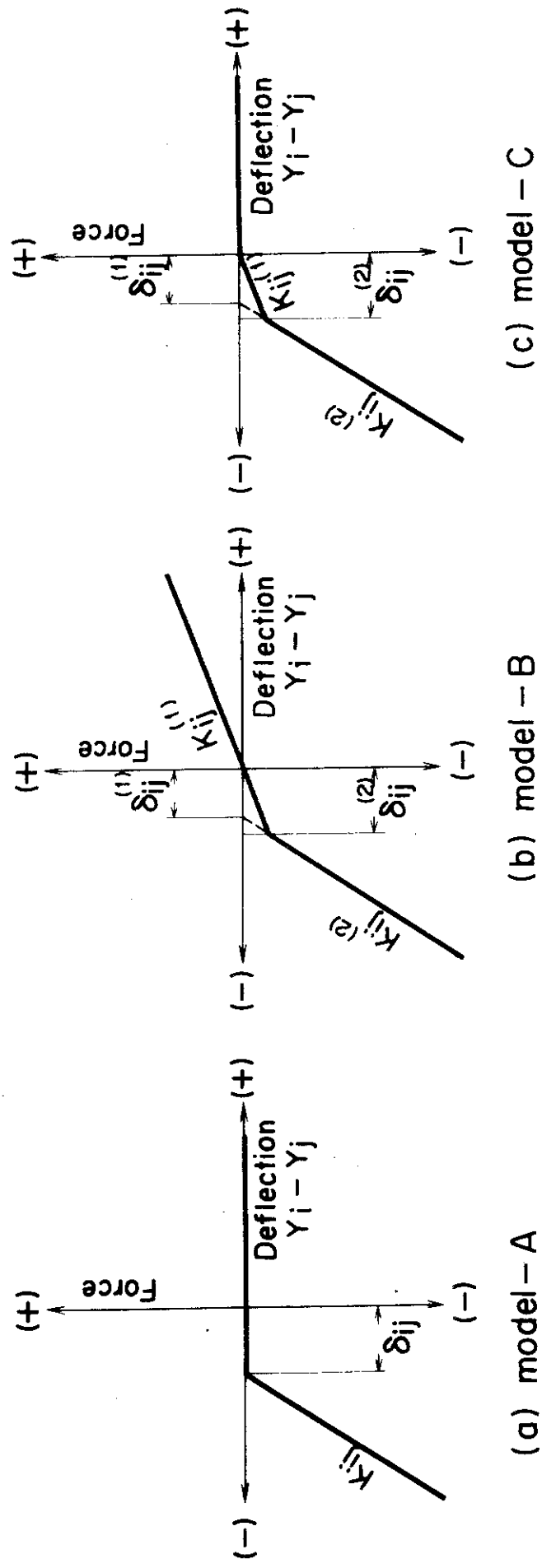

Fig. 8 Calculation model for discontinuous mass system

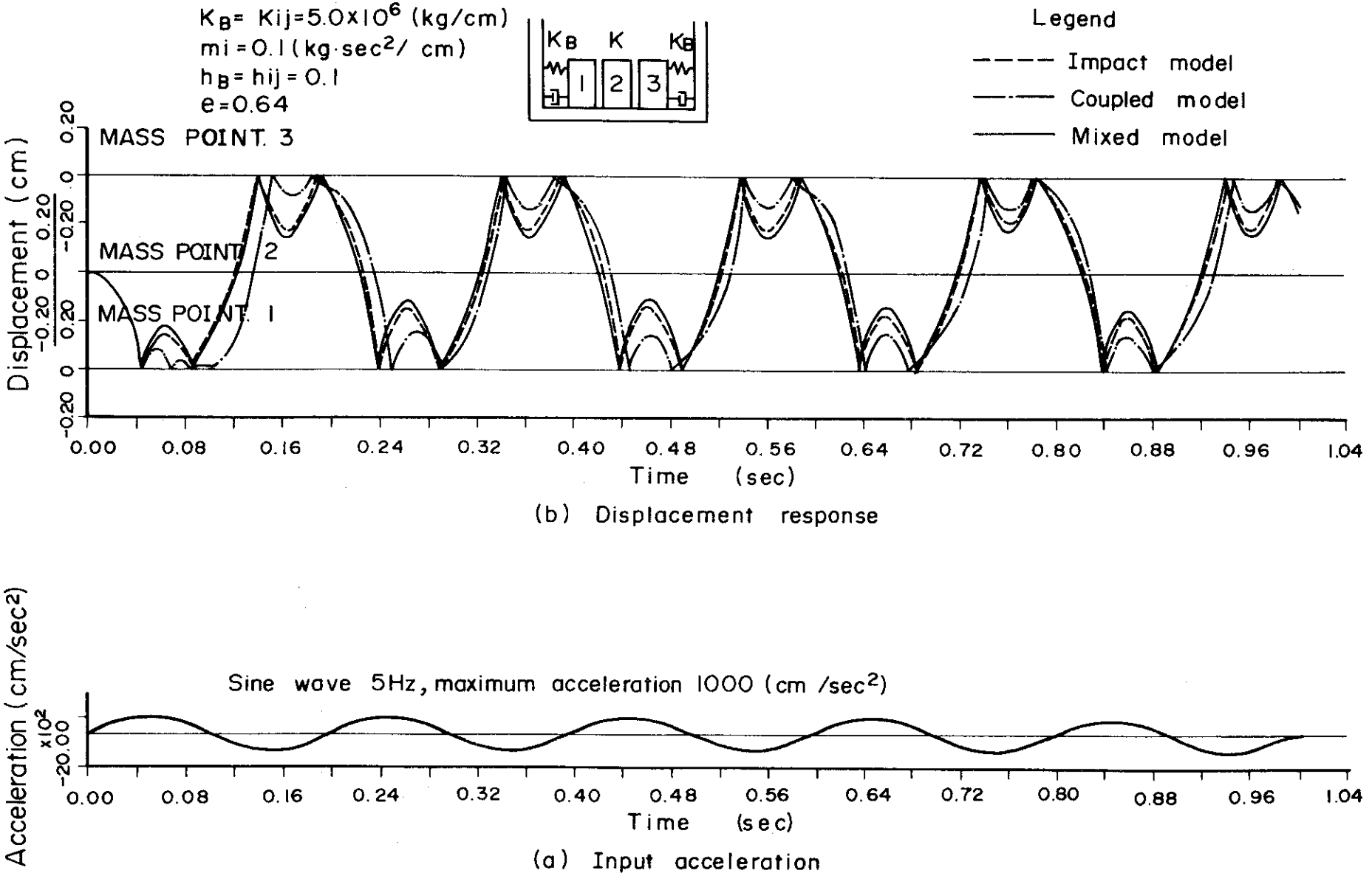

Fig. 9 Comparison of three impact model on response

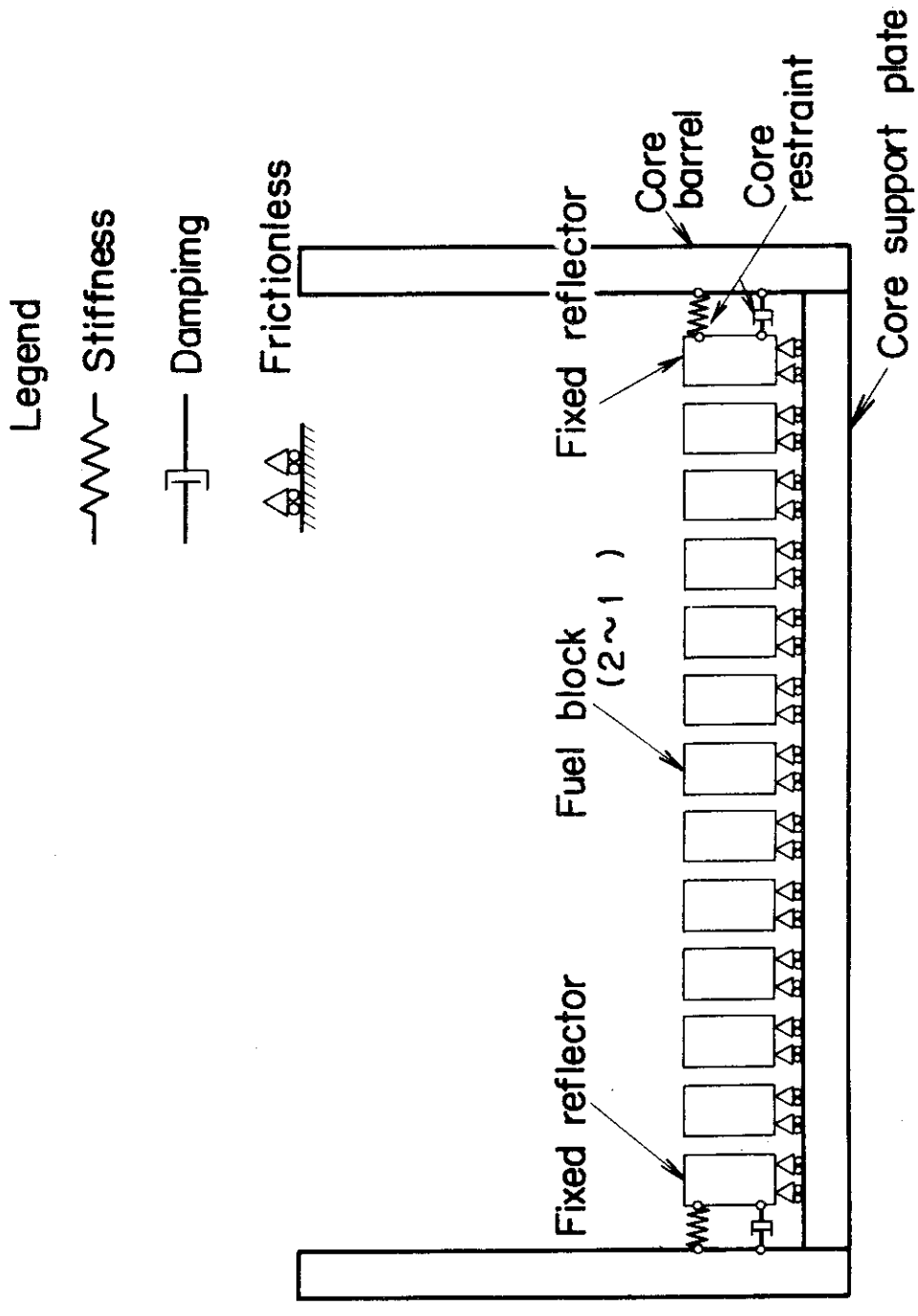

Fig. 10 1-D calculation model for seismic response analysis of HTGR core

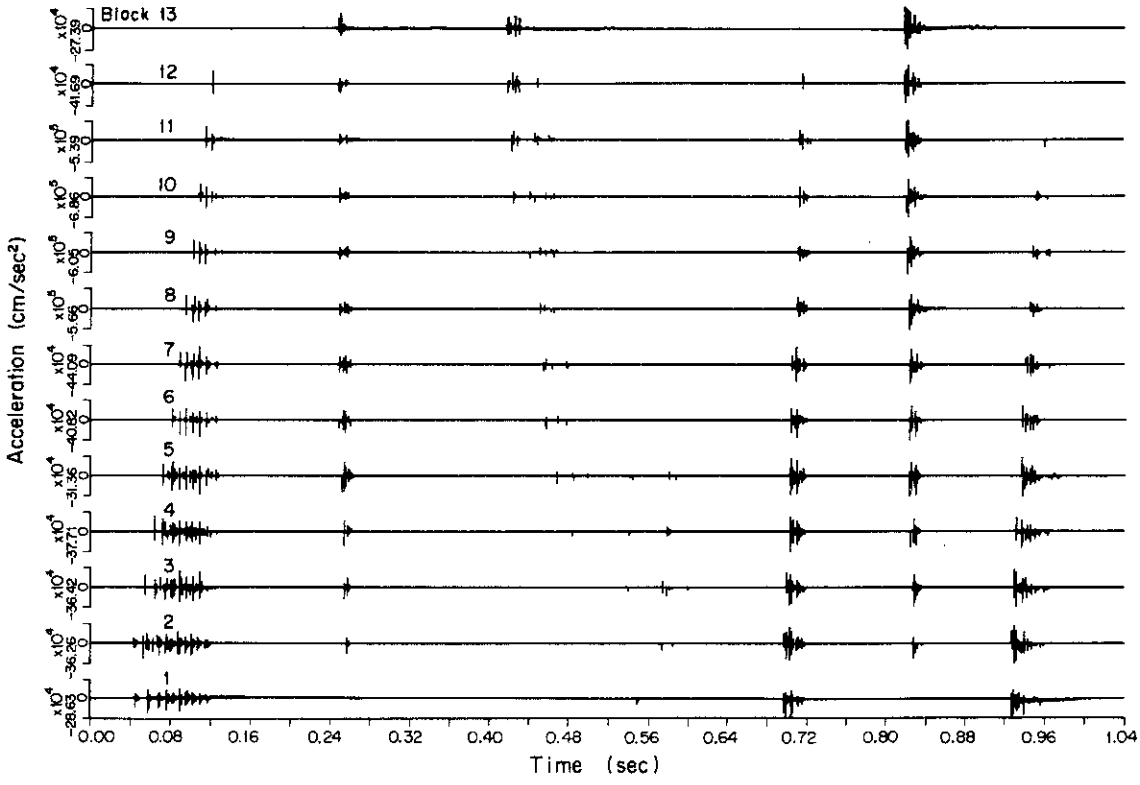

(c) Accelerantion response

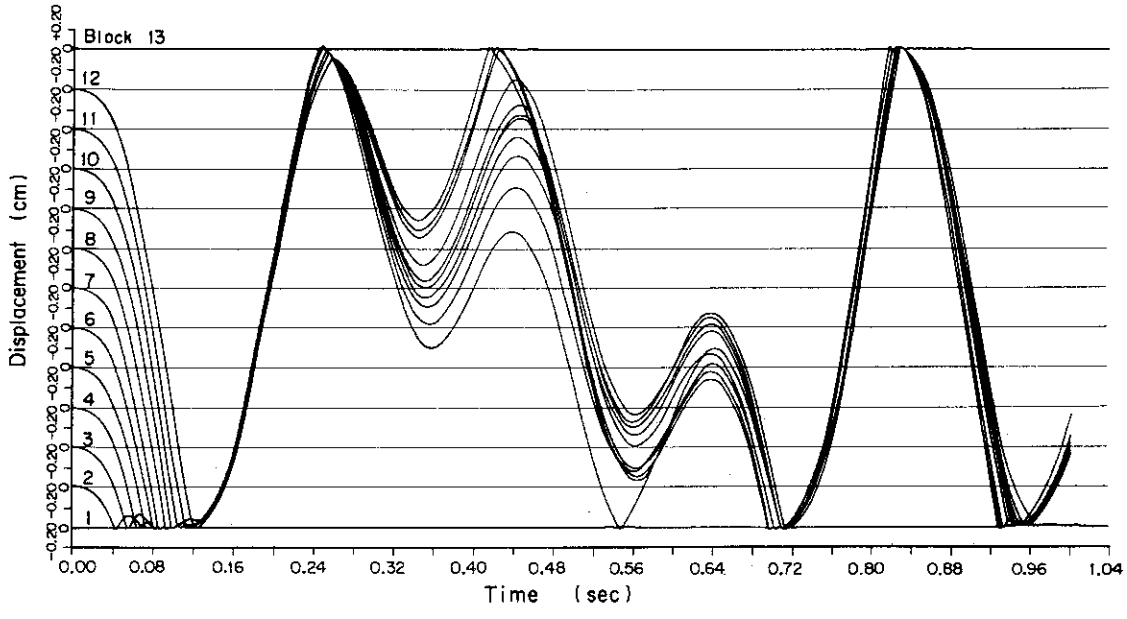

(b) Displacement response

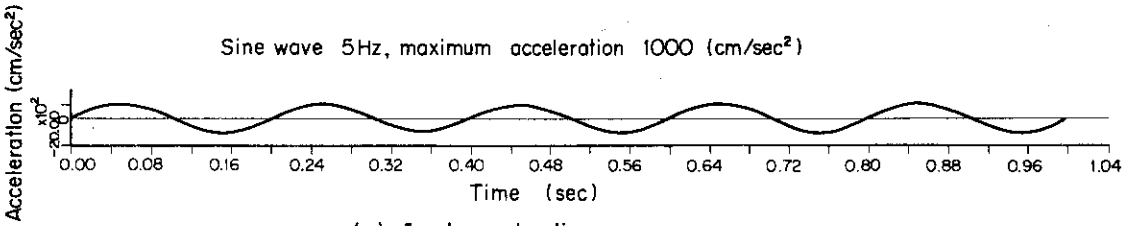

(a) Input acceleration

Fig. 11 Time-histories response of blocks

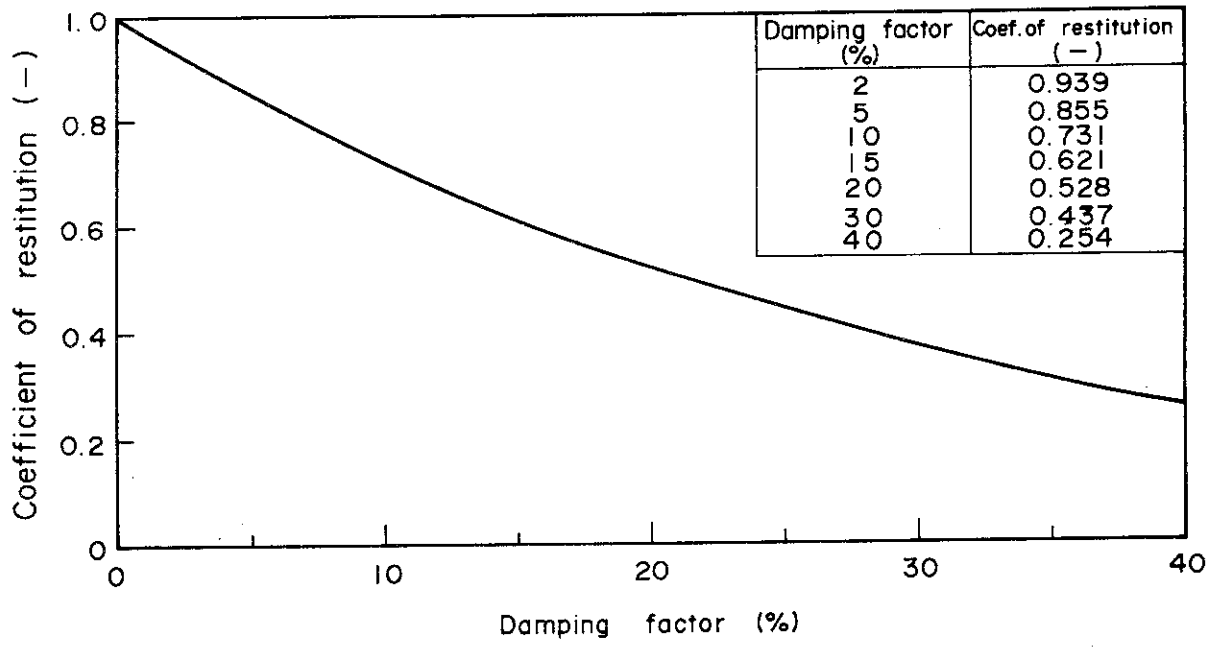

Fig. 12 Damping factor vs. coefficient of restitution

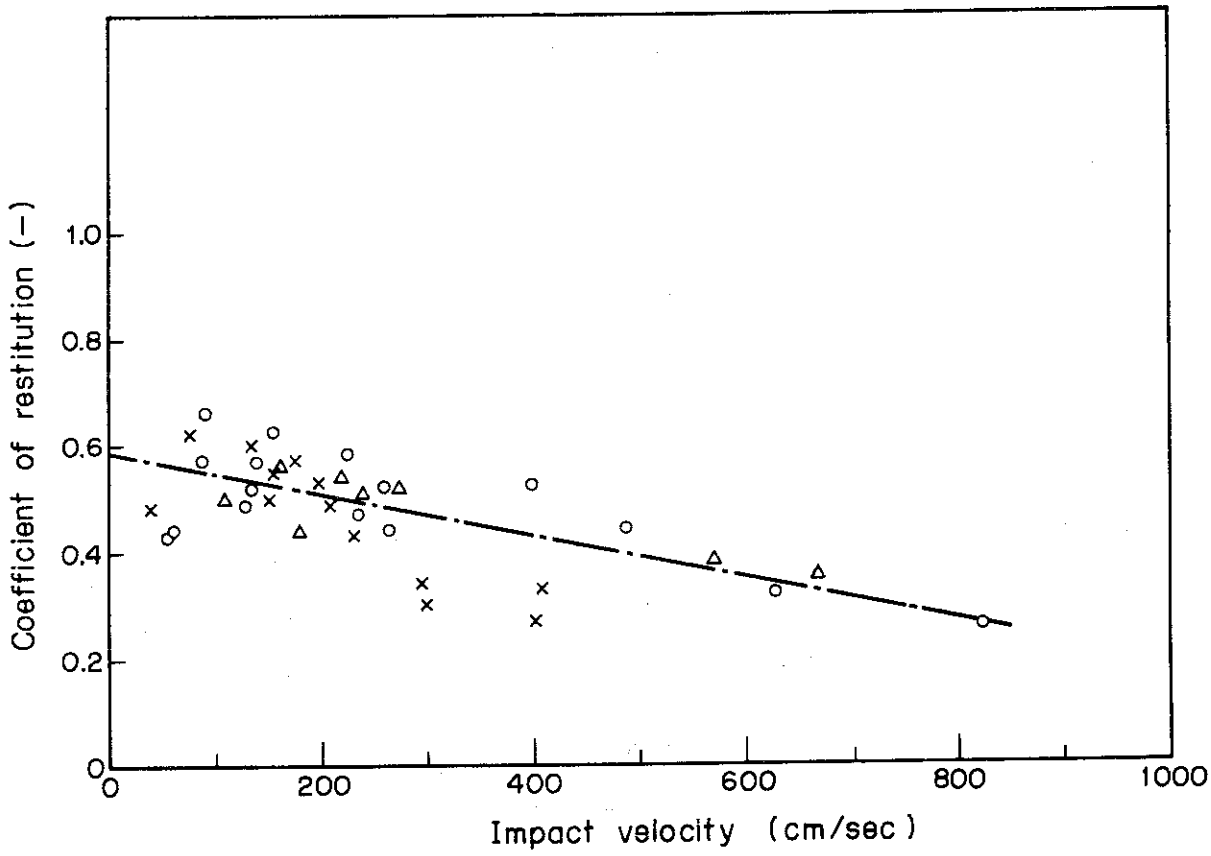

Fig. 13 Coefficient of restitution vs. impact velocity

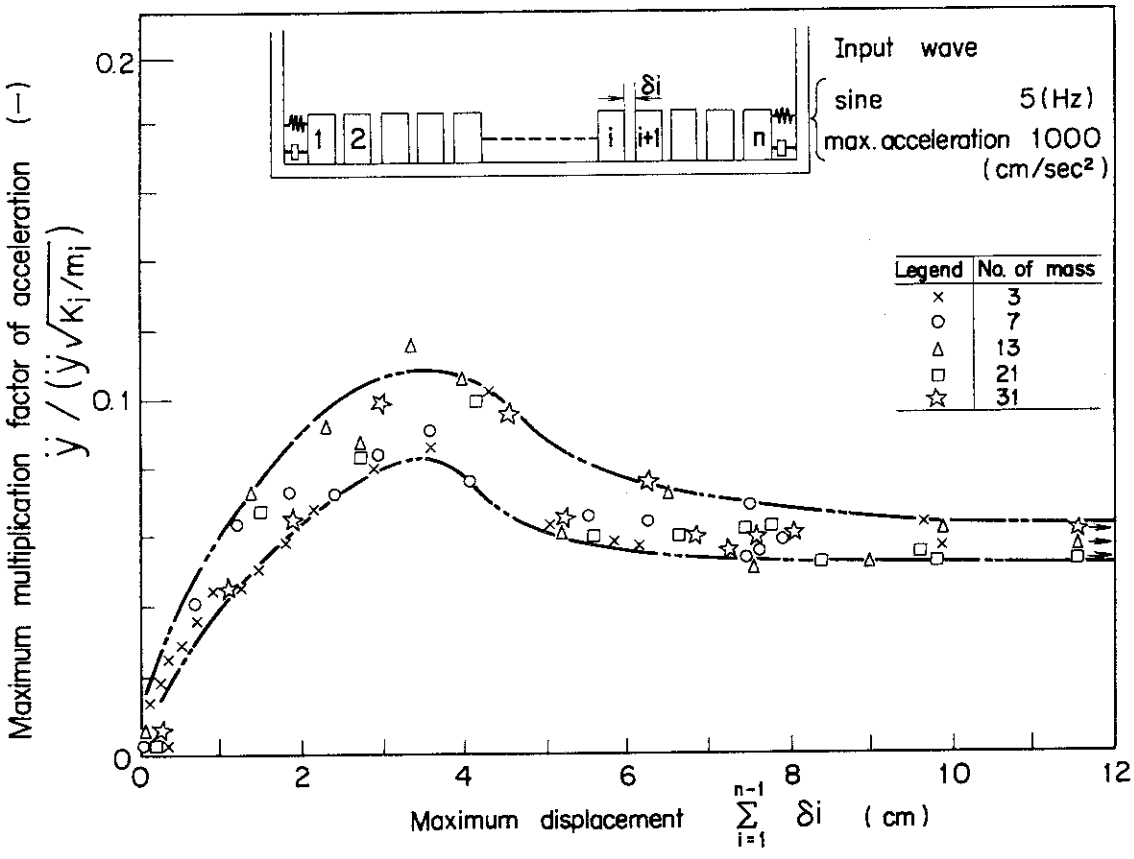

Fig. 14 Effect of mass points number on response

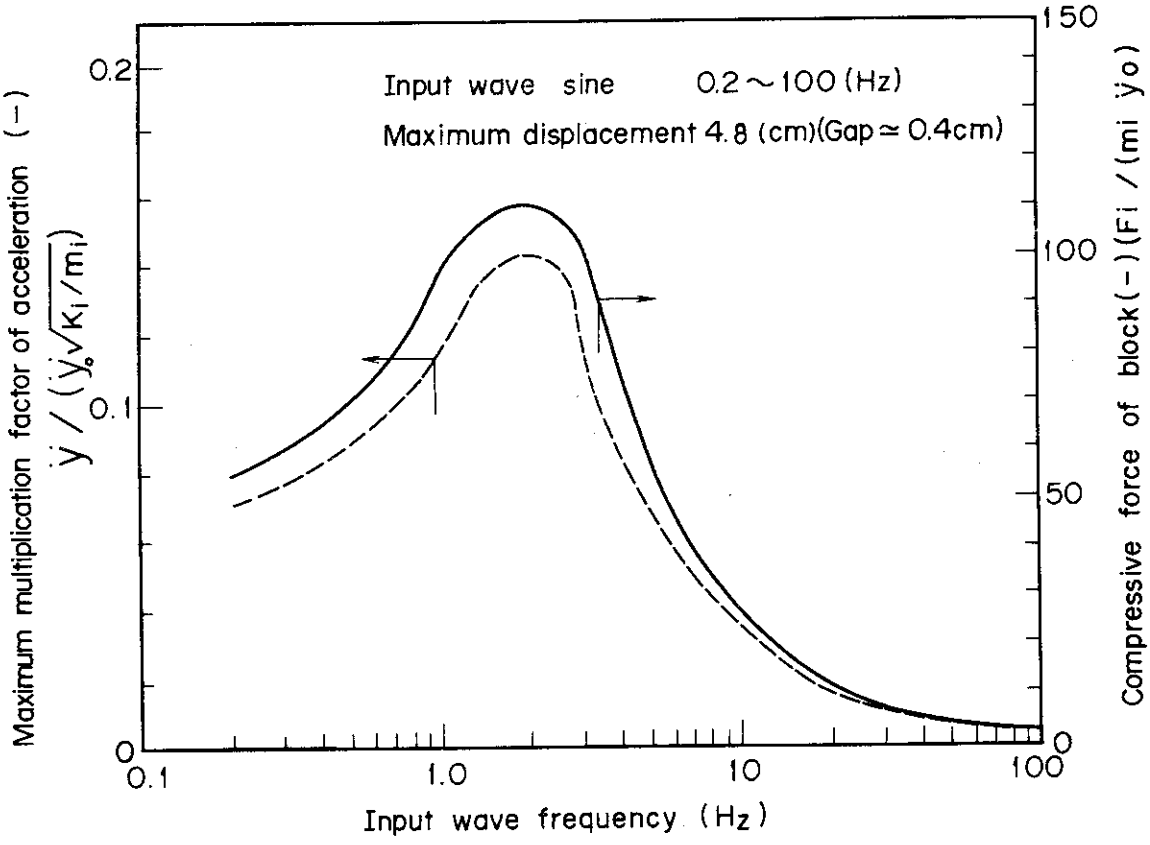

Fig. 15 Comparison between response acceleration and compressive force

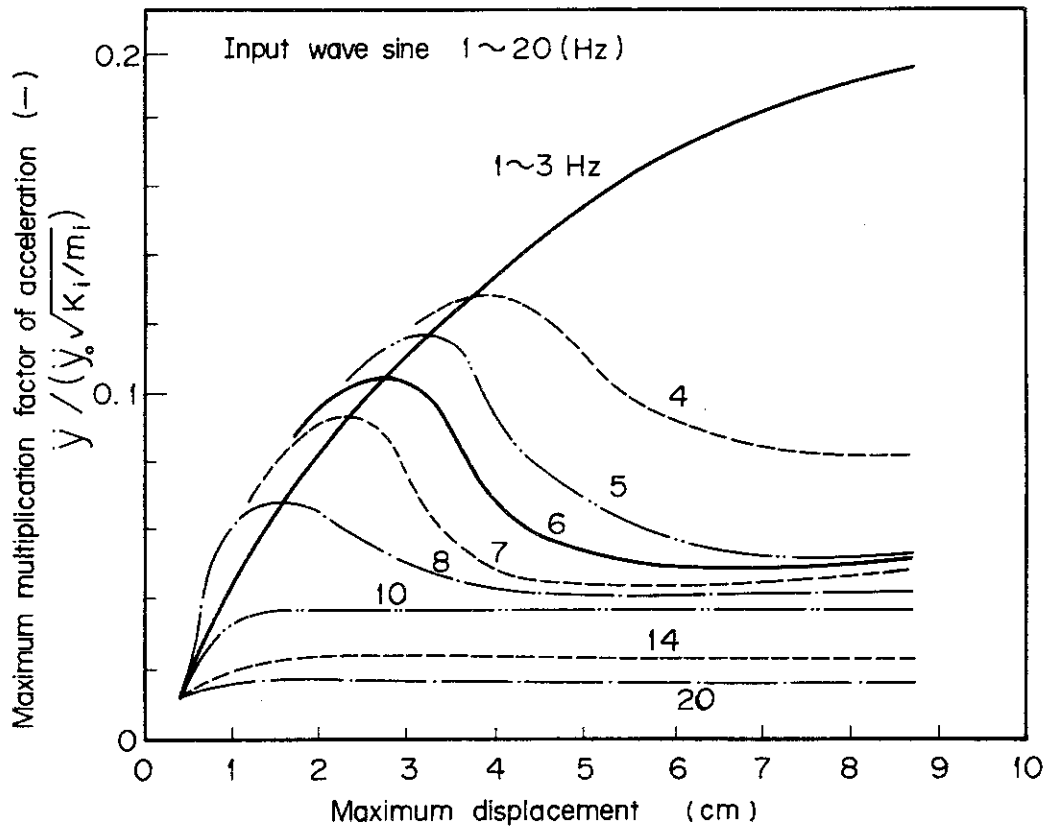

Fig. 16 Effect of maximum displacement on response

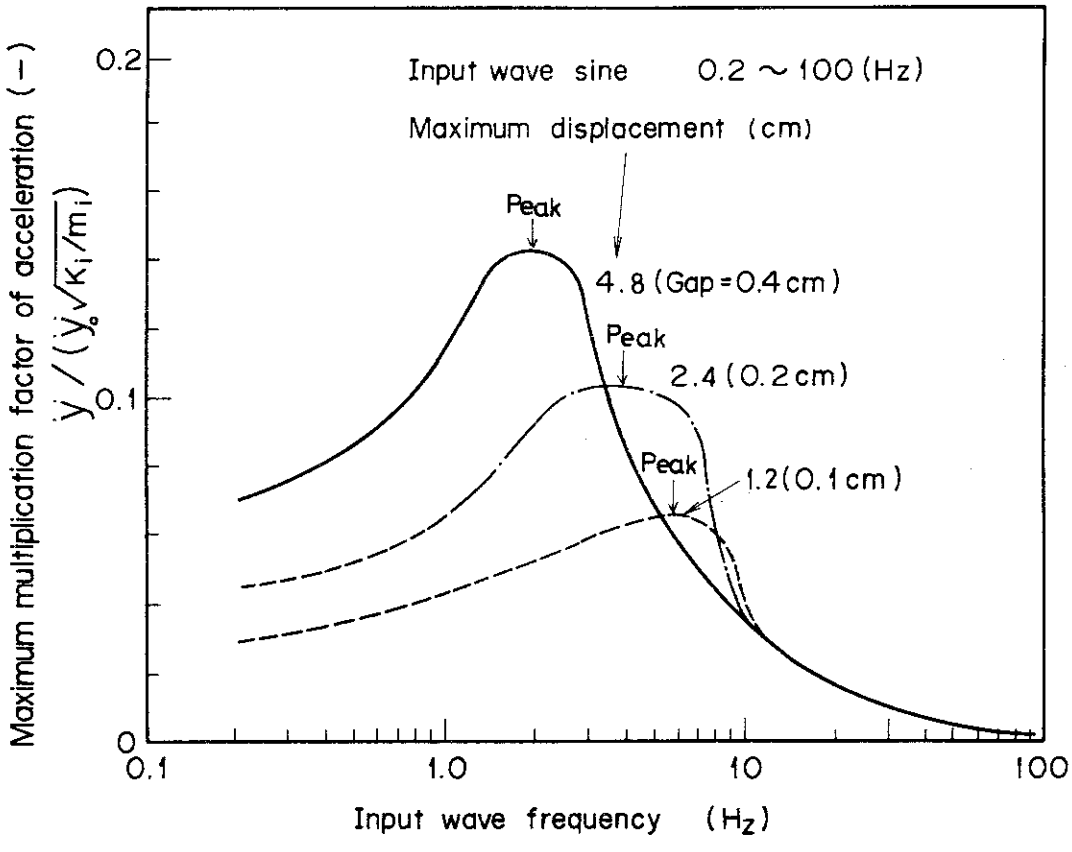

Fig. 17 Effect of input wave frequencies on response

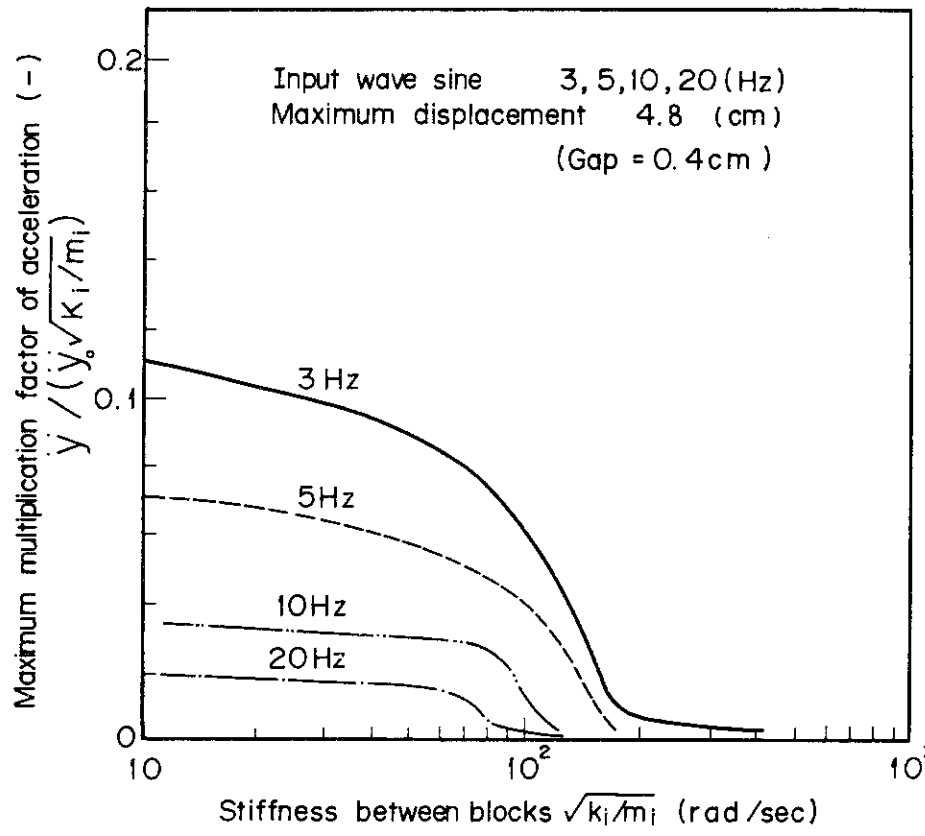

Fig. 18 Effect of stiffness between blocks on response

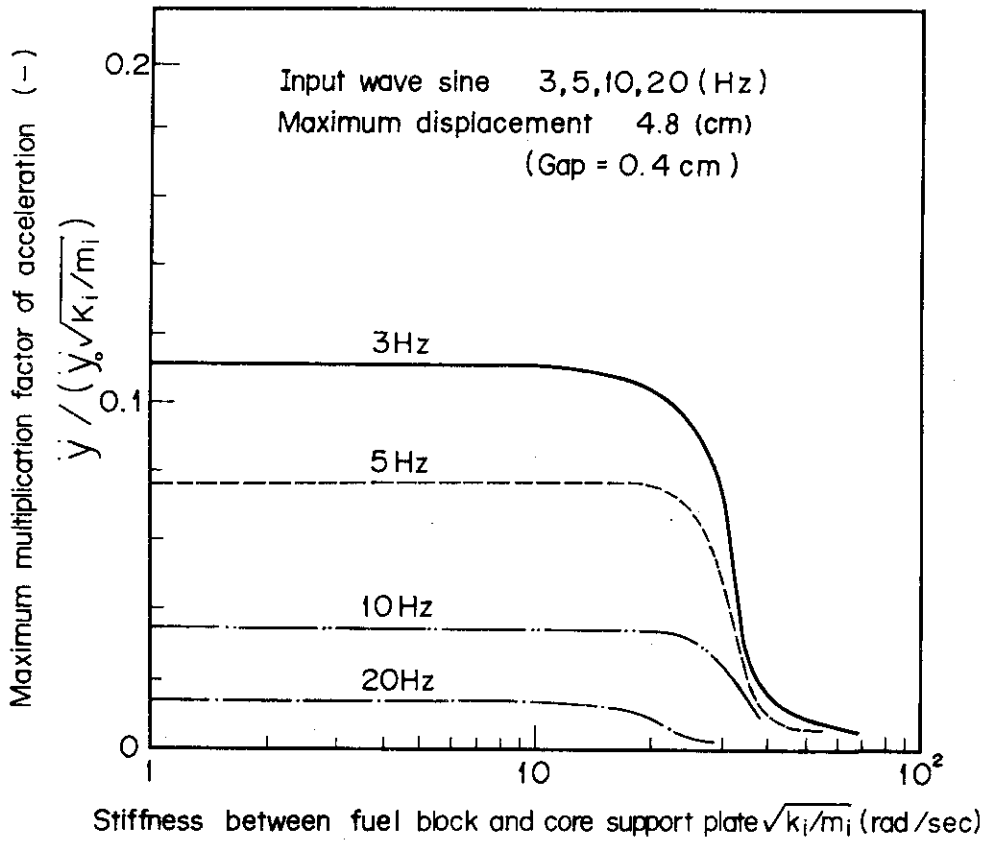

Fig. 19 Effect of stiffness between block and support plate on response

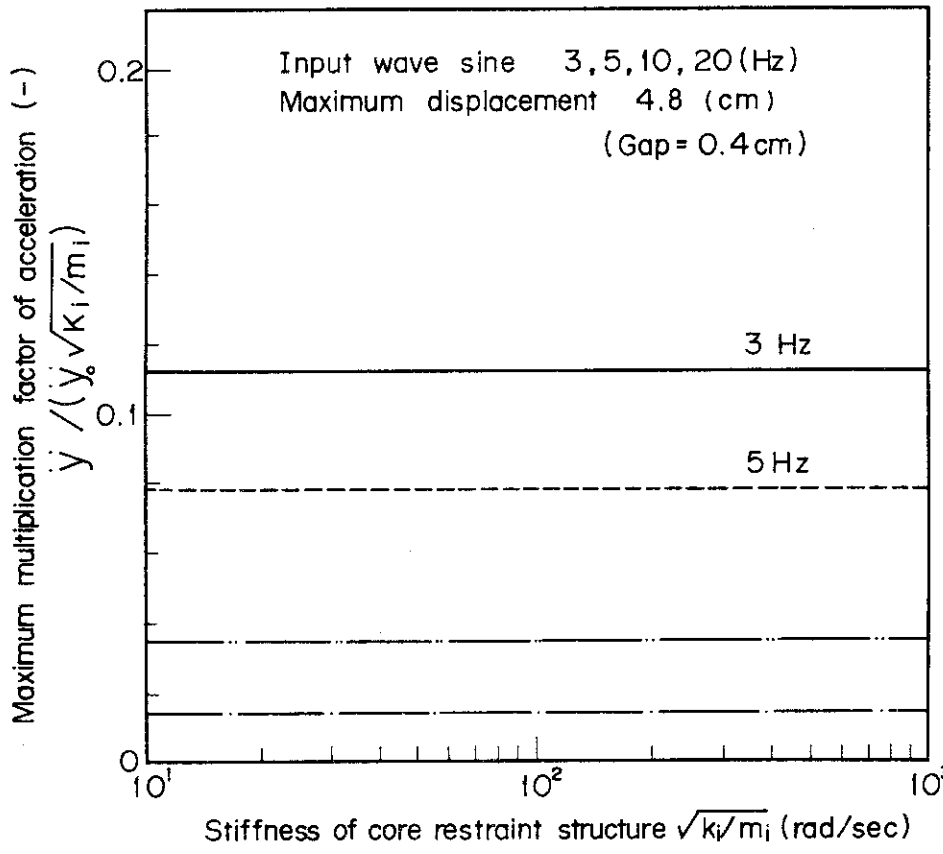

Fig. 20 Effect of core restraint structure on response

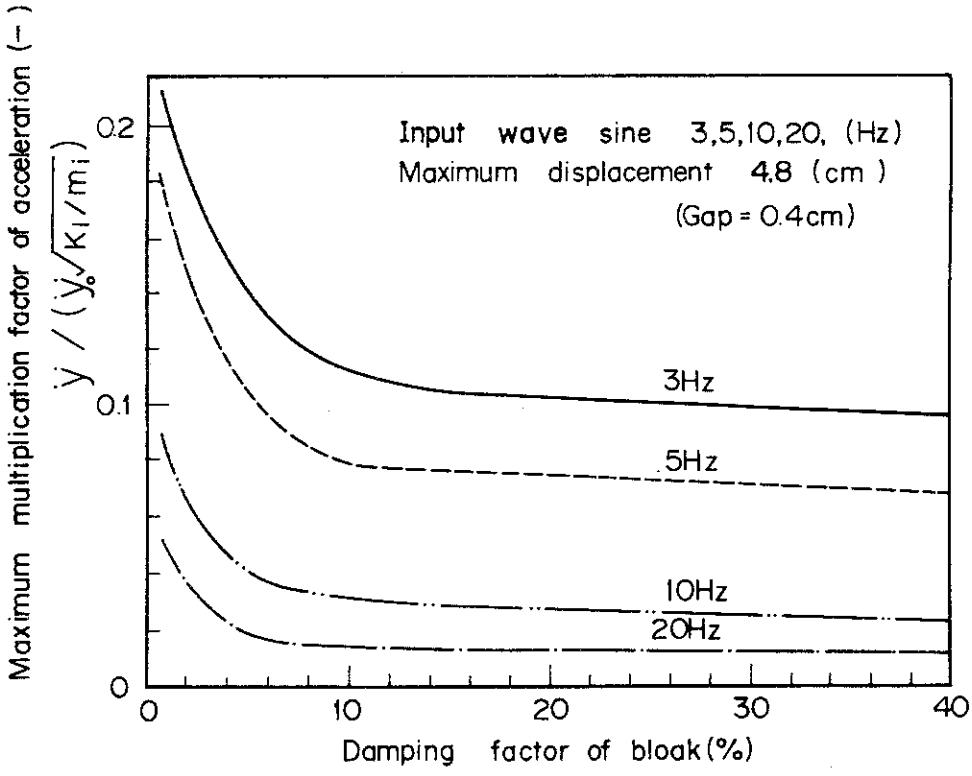

Fig. 21 Effect of block damping on response

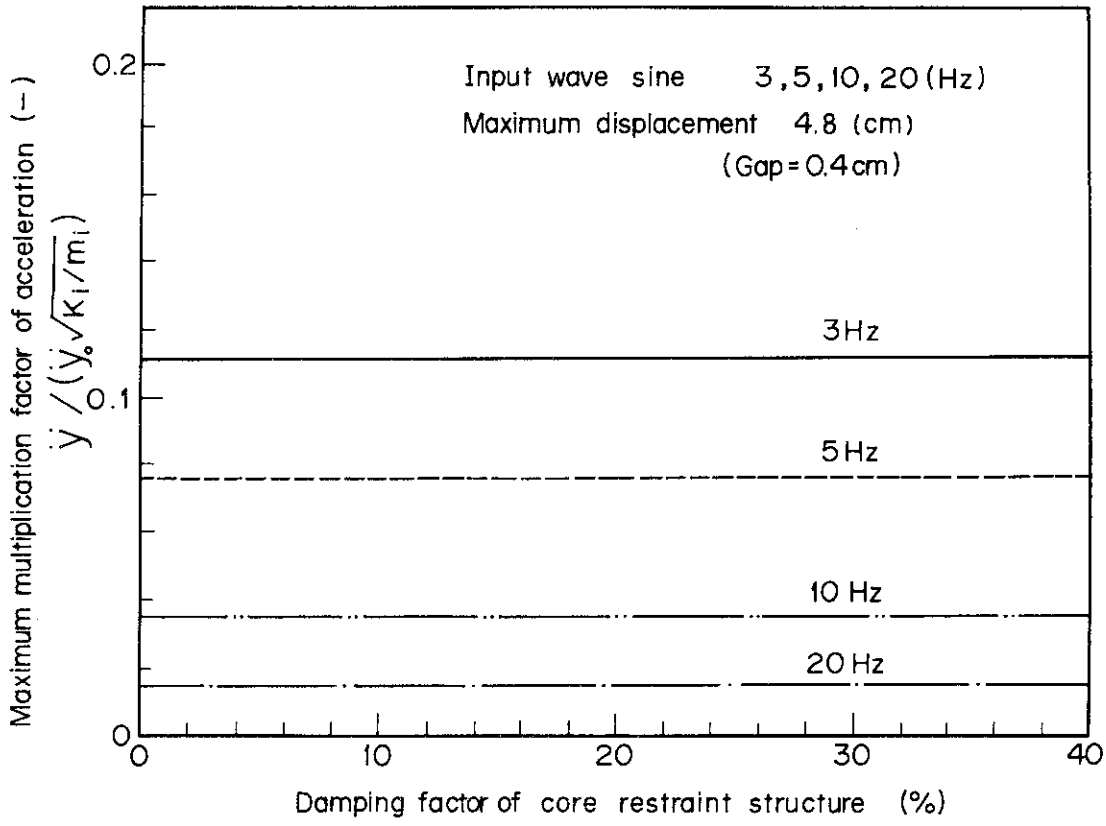

Fig. 22 Effect of restraint-structure damping factor on response

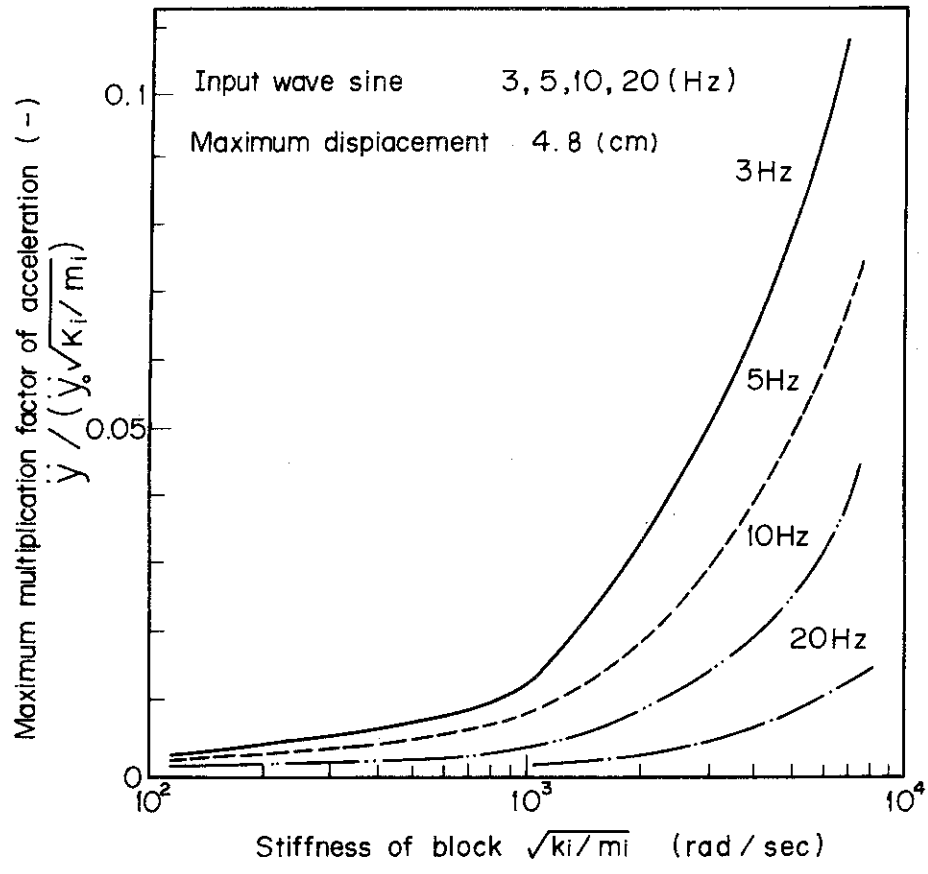

Fig. 23 Effect of block stiffness on response

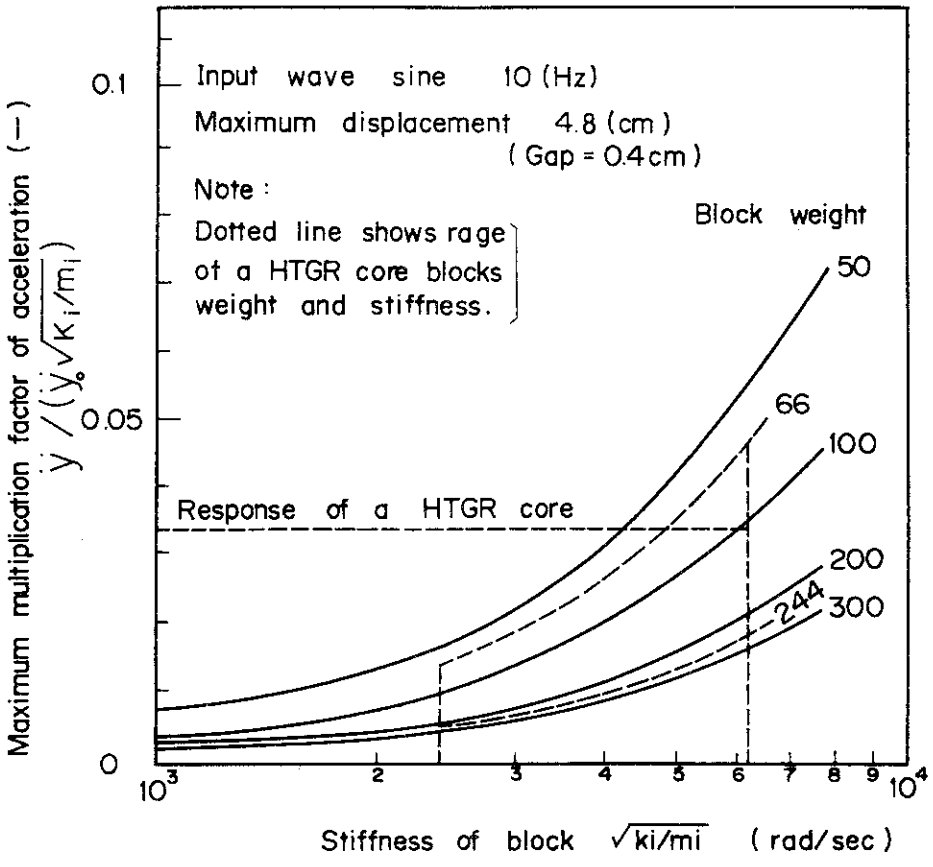

Fig. 24 Effect of random mass and stiffness

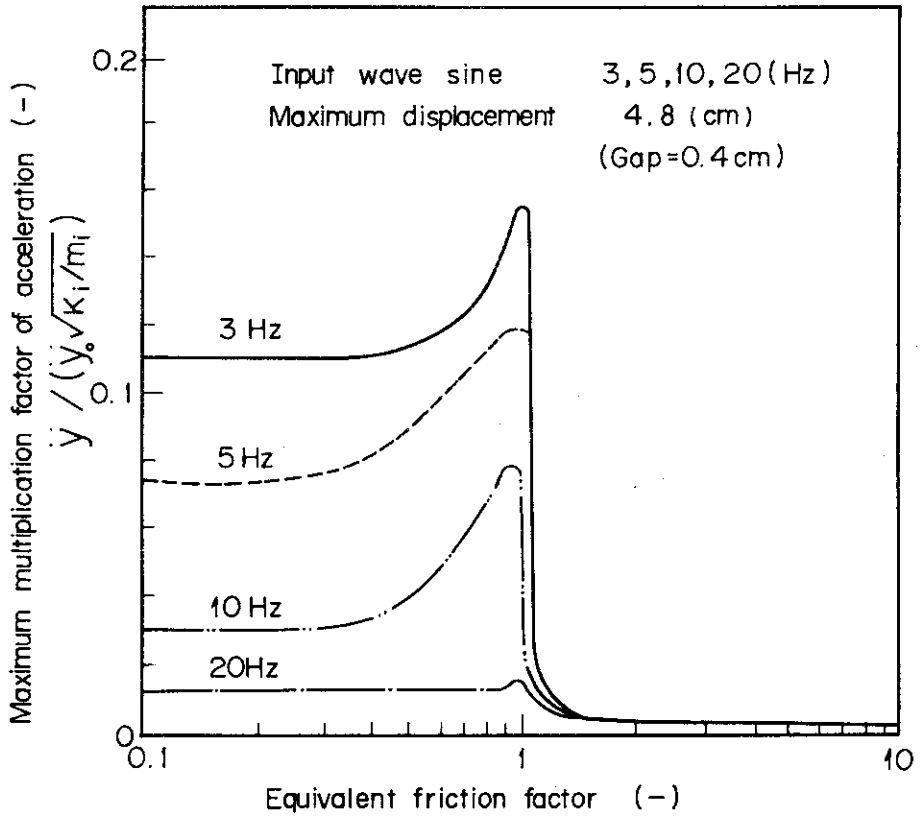

Fig. 25 Effect of friction factor on response